Self-assembly of binary nanoparticle dispersions: From square arrays and stripe phases to colloidal corrals

2009 Europhys. Lett. 85 56004

(http://iopscience.iop.org/0295-5075/85/5/56004)

A Letters Journal Exploring the Frontiers of Physics

March 2009

EPL, **85** (2009) 56004
doi: 10.1209/0295-5075/85/56004

www.epljournal.org

Self-assembly of binary nanoparticle dispersions: From square arrays and stripe phases to colloidal corrals

C. I. Mendoza[(a)] and E. Batta

Instituto de Investigaciones en Materiales, Universidad Nacional Autónoma de México - Apdo. Postal 70-360, 04510 México, D.F., Mexico

received 15 January 2009; accepted 19 February 2009
published online 20 March 2009

PACS 64.75.Yz – Self-assembly
PACS 82.70.Dd – Colloids
PACS 82.35.Jk – Copolymers, phase transitions, structure

Abstract – The generation of nanoscale square and stripe patterns is of major technological importance since they are compatible with industry-standard electronic circuitry. Recently, a blend of diblock copolymer interacting via hydrogen bonding was shown to self-assemble in square arrays. Motivated by those experiments we study, using Monte Carlo simulations, the pattern formation in a two-dimensional binary mixture of colloidal particles interacting via isotropic core-corona potentials. We find a rich variety of patterns that can be grouped mainly in aggregates that self-assemble in regular square lattices or in alternate strips. Other morphologies observed include colloidal corrals that are potentially useful as surface templating agents. This work shows the unexpected versatility of this simple model to produce a variety of patterns with high technological potential.

It has been a challenge in nanotechnology to produce highly ordered structures by controlling the position of nanoparticles over an extended length scale [1]; it is not easy to achieve this goal using direct micro- and nano-fabrication since such processes are prohibitively expensive and time-consuming below a certain length scale. As a result, the search of particles on the mesoscopic scales that self-organize into potentially useful structures by virtue of their mutual interactions is extremely important [2,3]. The ability of soft-matter systems to self-assemble in a surprisingly large variety of periodic arrangements has lead to use it as building blocks of bottom-up nanofabrication processes. This is a large and rapidly growing field of tremendous technological potential and fundamental interest that has been stimulated by the continuing progress in the manipulation of the interaction potentials between nanoparticles [4–8]. In particular, the self-assembly of nanometer-length-scale patterns in two dimensions is currently of interest as a method for improving throughput and resolution in nanolithography [9]; however, traditional self-assembling approaches based on block copolymer lithography spontaneously yield nanometer-sized hexagonal structures that are incompatible with the square arrangements used in industry-standard circuits [8]. That is the reason why among the targeted morphologies, stripes and square arrays are particularly important for the manufacture of microelectronic components since they would enable simplified addressability and circuit interconnection in integrated-circuit nanotechnology. There have been theoretical efforts to tailor interparticle interactions to spontaneously produce target many-particle configurations for single-component systems [2,3] but the optimized potentials found are difficult to fit by available interactions. Recently, an experimental technique based on a blend of diblock copolymers was developed to produce nanoparticles that assemble into square arrays [8]. The blend consists of two kinds of diblock copolymers, A-B and B′-C, being the A and C blocks mutually repulsive and incompatible with blocks B and B′. Block B contains small numbers of groups that form hydrogen bonds to complementary groups in block B′ (fig. 1a). The attractive interactions between complementary hydrogen bonds suppress macrophase separation in favor of microphase separation, thereby producing large-scale assembly of nanoscale features. By controlling the amount of hydrogen bonding units, the molecular weights and compositions of the block copolymers, diverse families of ordered structures are achieved, including square arrays of cylinders that are the result of the competition

(a)E-mail: cmendoza@iim.unam.mx

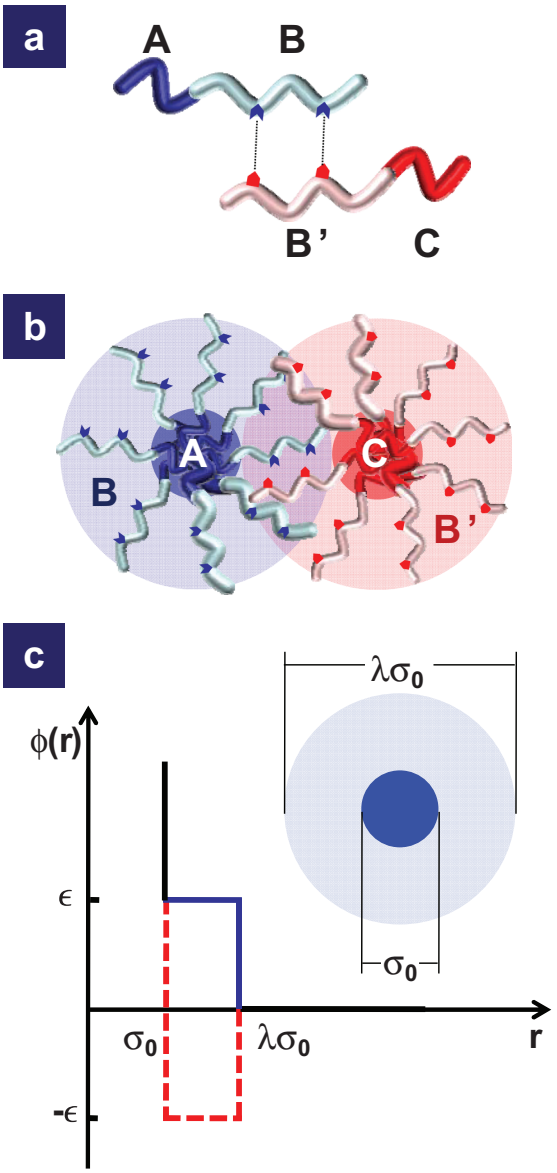

Fig. 1: (Colour on-line) Description of the model. (a) Two kinds of diblock copolymer, A-B and B′-C. Block B contains small numbers of groups (blue) that form hydrogen bonds to complementary groups (red) in block B′. (b) Schematic representation of the blend of block copolymer with hydrogen-bond interactions forming cylindrical micelles (top view). (c) The interaction between a pair of cylindrical micelles is modeled by a hard-core soft-corona potential. If the micelles are of the same component, then the corona is a square shoulder, otherwise the corona is a square well.

between the different interactions (see fig. 3 of ref. [8]). Inspired by these experiments, we propose a simple model system that reproduces such structures as a result of a binary mixture of nanoparticles interacting via isotropic short-ranged competing potentials. The model we propose treats the interactions between the block copolymers in an effective way that takes into consideration the entropy of the brush-like coronas surrounding each cylinder via a soft repulsive shoulder and the hydrogen bonding via a square-well attraction. Such simple pair potentials are often used to describe effective interactions among substances with supramolecular architecture [10,11]. We consider a two-dimensional (2D) assembly of particles consisting of a hard core surrounded by a soft corona which is repulsive for particles of the same species and attractive otherwise. The simplicity of the model allows to predict, based on geometrical arguments, under which circumstances a given family of structures is obtained. Among the rich variety of patterns encountered, we can highlight the formation of square arrays and stripe phases for equimolar mixtures and the formation of colloidal corrals for asymmetric mixtures. These results suggest a strategy for producing a range of self-assembled structures which could be exploited for use as templating or directing agents in materials syntheses. Although we are primarily interested in the crystalline structures at low temperatures, we find that at higher temperatures the system presents a transition from an isotropic fluid phase to a disordered fluid-like stripe phase.

Our model is not limited to the above-mentioned diblock copolymer blend since core-corona architectures are also present in numerous physical systems such as dendritic polymers, hyper-branched star polymers, etc. Among these are, for instance, colloidal particles with block-copolymers grafted to their surface where self-consistent field calculations lead to effective interactions that can be modeled by a square-shoulder potential [12]. Such interactions can be controlled by adjusting the length, species, the grafting density of the grafted polymers, the quality of the solvent, the density and location of the hydrogen bonding, etc. Numerical simulations have shown that single-component softened-core repulsive potentials may give rise to strip phases [12–17] and periodic structures that are explained in terms of the competing interactions between the hard core and the soft shoulder. Our aim is to study the influence that the introduction of a second component has in the domain formation. The second component interacts attractively with the first one in order to suppress macroscopic phase separation. This attractive interaction models the hydrogen bond attraction between B and B′ segments of the diblock copolymer system of ref. [8]. When this system forms cylindrical micelles, as shown schematically in fig. 1b, then our model treats them as nanoparticles with a core-corona architecture where the hard core represents the blocks A and C and the soft corona models the effective interactions between the blocks B and B′. Therefore, our system consists of a binary mixture of particles interacting through a radially symmetric pair potential composed by an impenetrable core of diameter σ_0 with an adjacent square shoulder with range $\lambda\sigma_0$ (fig. 1c), *i.e.*,

$$\phi(r) = \begin{cases} \infty, & r \leqslant \sigma_0, \\ \pm\epsilon, & \sigma_0 < r < \lambda\sigma_0, \\ 0, & r \geqslant \lambda\sigma_0, \end{cases} \tag{1}$$

r being the pair distance. Particles of the same component interact through the repulsive shoulder ϵ, whereas particles of different species interact through the attractive potential well of depth $-\epsilon$. The model intend to represent the interactions of the block copolymers of ref. [8] as long as they form cylindrical micelles (fig. 1b). At large distances, the particles do not overlap and the interaction vanishes, the repulsive shoulder models the steric repulsion between blocks B or between blocks B′ due to the overlap of the brush-like coronas, and the attractive well models the hydrogen bonding between blocks B and B′. Finally, at small separations penetration of the compact cores is very unfavorable and gives rise to the hard-core repulsion. The simple functional form of the interaction potential not only captures the essential features of colloidal particles with core-corona architecture, it also offers many computational advantages and allows to understand, using simple geometrical considerations the system's self-assembly strategy [18]. Standard Monte Carlo simulations based on the canonical ensemble (NVT simulations) in a square box of side L with periodic boundary conditions have been carried out using the Metropolis algorithm. We have used σ_0 and ϵ as length and energy units, respectively and we have studied the pattern formation dependence on λ, reduced temperature $T^* = k_B T/\epsilon$, where k_B is Boltzmann's constant; reduced number density $\rho^* = N\sigma_0^2/L^2$, and relative amount of each species $x = N_2/N_1$, with N_i the number of particles of species i and $N = N_1 + N_2$ the total number of particles. Simulations are performed with $N = 1000$ particles (runs with $N = 4000$ were done for the largest value of λ). In all cases, the system is first disordered at high temperature and then brought from $T^* = 1$ ($T^* = 10$ for the largest value of λ) to the final temperature $T^* = 0.1$ through an accurate annealing procedure with steps of 0.01 (0.1 for the largest value of λ). An equilibration cycle consisted, for each temperature, of at least 2×10^6 MC steps, each one representing one trial displacement of each particle, on average. At every simulation step a particle is picked at random and given a uniform random trial displacement within a radius of $0.5\sigma_0$.

A variety of interesting structural features of this simple model at low temperatures are in evidence in fig. 2, where a few of them are exhibited. Panel (a) shows a representative example of the spatial configuration that the system adopts for $\lambda = 1.5$, $\rho^* = 0.5$, and $x = 1$. We observe that the system self-assemblies forming an aggregate made of an alternating square array of particles with a lattice parameter determined by the range of the soft coronas (inset fig. 1a). The system adopts this array in order to maximize the number of favorable overlaps between particles of different species avoiding at the same time unfavorable overlaps between particles of the same type. Thus, this simple model reproduces qualitatively well the main characteristic of the block copolymer system of ref. [8], *i.e.*, the fundamentally and technologically important result that this system self-assemblies forming square arrays. Unlike systems with only one component [14], the ratio between the hard and soft cores is critical even if they are comparable to each other since different patterns may appear by just changing the value of λ. In fig. 2b we show the structures obtained for the same set of parameters as in fig. 2a except that the value of λ has been increased to $\lambda = 2$. The particles now form aggregates in which the particles prefer to align forming intercalated stripes of alternating species. Each stripe consists of only one type of particles and try to avoid overlap between the coronas of neighboring stripes of the same species, thus, the shoulder width act as

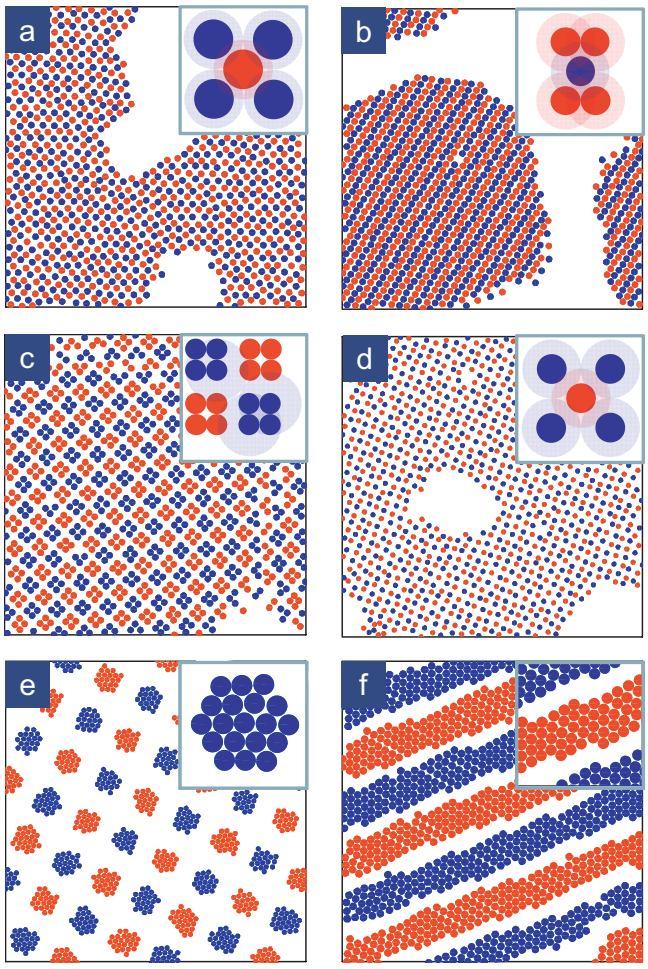

Fig. 2: (Colour on-line) Spatial arrangements of the system at temperature $T^* = 0.1$ for an equimolar mixture $x = 1$. (a) Square array formed in a system with $\lambda = 1.5$ and $\rho^* = 0.5$, (b) stripe phase obtained for $\lambda = 2$ and $\rho^* = 0.5$, (c) a square array of tetrameres appears for $\lambda = 3$ and $\rho^* = 0.5$, (d) square array obtained for $\lambda = 2$ and $\rho^* = 0.3$. Comparing panels (b) and (d) we see that at the lowest density shown the system aggregates in square arrays whilst at the largest density the system prefers to form stripes of alternating species. For very large values of λ, larger aggregates of hexagonal close-packed particles of the same species are formed. These aggregates in turn self-assemble in (e) square arrays for $\lambda = 10$ and $\rho^* = 0.3$, and (f) thick stripes for $\lambda = 10$ and $\rho^* = 0.65$.

spacer between neighboring stripes (see inset of fig. 2b). Increasing even more the range of the soft corona, the system develops a completely different strategy to form stable configurations giving rise to the appearance of new patterns. This is shown in fig. 2c where a pattern formed by a square array of tetrameres develops if λ is increased to $\lambda = 3$. Each square tetramer is formed by four close packed particles of the same species and the separation between the tetrameres is dictated by the condition that the coronas of each particle overlaps at most four coronas of particles of the same species, as shown in the inset of fig. 2c where we have highlighted the coronas that settle the spacing between tetrameres. Two lines of defects, one near the upper side and the second near the right side of the simulation cell are in evidence. They are originated in the periodic boundary conditions; effectively, the lattice of tetrameres extend over the entire length of the simulation cell and join up with their periodic images. Since this length is not commensurable with the periodicity of the lattice the defect lines appear. A few vacancies scattered along the lattice that could not be annealed out are also present, but this is to be expected for kinetic reasons. For very large values of λ ($\lambda = 10$ in figs. 2e and f), hexagonal close-packed aggregates of particles of the same species are formed and this aggregates in turn self-assemble in square arrays (panel (e)) or thick stripes (panel (f)) formed similarly of hexagonal close-packed particles (inset figs. 2e and f). We can think of the aggregates as larger interacting particles with the internal structure only changing the effective inter-aggregate interactions [16], thus the system try to arrange particles so that the shape of the cluster becomes as circular as possible. This, in turn, guarantees that the underlying structure is close to the energetically most favorable hexagonal lattice [17]. Within the lane structure (fig. 2f) the system follows a similar strategy consisting in first optimize the packing inside a stripe, leading to hexagonal particle arrangements inside each lane. Nevertheless, due to the increasing complexity of the inner structure of the patterns, a simple energetic explanation in terms of overlapping coronas is very difficult.

Let us stress that the attraction between different species not only causes the alternation of the different species in the lattices. It also gives rise to structures that are not present in the homogeneous system and viceversa. For example, a square lattice is not present in the single-component case with the shoulder range used in fig. 1a, as shown in ref. [17]. On the other hand, the ideal hexagonal lattice exhibited in the homogeneous case is not present in the binary mixture for the same shoulder range. Similarly, a square array of square tetrameres has not been observed in the single-component system. Thus, the additional requirement of maximizing favorable overlaps in the binary mixture leads to different self-assembly strategies.

In our model, configurational energy is essentially determined by geometry; thus, simple geometrical considerations can be used to predict the parameters at which a given pattern is expected to be adopted at zero temperature. For values of the range of the soft coronas such that $\lambda \geqslant \sqrt{2}$ the lattice constant a at $T^* = 0$ is determined by the condition that the soft coronas of the nearest-neighbors of the same species just touch as shown in the inset of fig. 2a. Therefore, the lattice parameter takes the value $a = \lambda\sigma_0$ and the density of the aggregate is $\rho^*_{\text{squares}} = 2/\lambda^2$. On the other hand, if $\lambda < \sqrt{2}$, then the particle hard cores just touch forming a close packed square array whose lattice constant $a = \sqrt{2}\sigma_0$ is determined by the hard-core diameter σ_0 and the density of the aggregate is $\rho^*_{\text{squares}} = 1$. The energy per particle of this array is $u = -4\epsilon$ which is the number of overlaps between the corona of a given particle and its first neighbors times the energy of each overlap. The square array has the characteristic that no overlap between the coronas of particles of the same component takes place. However, if the density is so high that the coronas of particles of the same species have not enough space to accommodate without overlapping, then the system adopts a different strategy in order to minimize its energy; the formation of lanes provides the energetically best solution. This is achieved (if $\lambda \geqslant 2$) when the soft corona of a given particle just touch the ones of the second nearest neighbors of the same stripe determining the separation between the particles in the same stripe. On the other hand, if $\lambda < 2$, neighboring particles of the same stripe are in direct contact, forming a one-dimensional close-packed arrangement. As a result, in both cases, the particles form a centered rectangular arrangement as shown in the inset of fig. 2b, with the lattice parameter in the direction of the stripe given by $a = \lambda\sigma_0/2$ if $\lambda \geqslant 2$ or $a = \sigma_0$ if $\lambda < 2$. The lattice parameter perpendicular to the stripes is given by the distance between adjacent stripes of the same species which are separated by a distance $b = \lambda\sigma_0$ if $\lambda \geqslant \sqrt{3}$ or $b = \sqrt{2}\sigma_0$ if $\lambda < \sqrt{3}$. The densities are, correspondingly, $\rho^*_{\text{stripes}} = 4/\lambda^2$ if $\lambda \geqslant 2$, $\rho^*_{\text{stripes}} = 2/\lambda$ if $\sqrt{3} \leqslant \lambda < 2$, and $\rho^*_{\text{stripes}} = 2/\sqrt{3} \simeq 1.1547$ if $\lambda < \sqrt{3}$; the last situation corresponds to a hexagonal close packing. Using similar geometrical considerations we obtain the energy per particle in each case, $u = -6\epsilon$ if $\lambda \geqslant \sqrt{3}$ or $u = -2\epsilon$ if $\lambda < \sqrt{3}$. Finally, for the square array of tetramers the lattice parameter is $a = \sigma_0/\sqrt{2}(1 + \sqrt{2\lambda^2 - 1})$ if $\lambda \geqslant \sqrt{5}$ and the corresponding density is $\rho^*_{\text{tetramers}} = 16(1 + \sqrt{2\lambda^2 - 1})^{-2}$. When $\lambda < \sqrt{5}$ the particles of the adjacent tetramers touch their hard cores forming a square close packing and therefore $\rho^*_{\text{tetramers}} = 1$. The energy per particle of this array is given by $u = -8\epsilon$ if $\lambda \geqslant \sqrt{5}$, $u = -4\epsilon$ if $2 \leqslant \lambda < \sqrt{5}$, or $u = 0$ if $\lambda < 2$.

By comparing to each other the energies of the lattices found previously, it is possible to construct a phase diagram at zero-temperature which allows to predict the structures adopted for a given set of parameters. Regions of the phase diagram where minimum energy configurations at $T^* = 0$ appear are shown in fig. 3 for the three simplest structures obtained in the simulations.

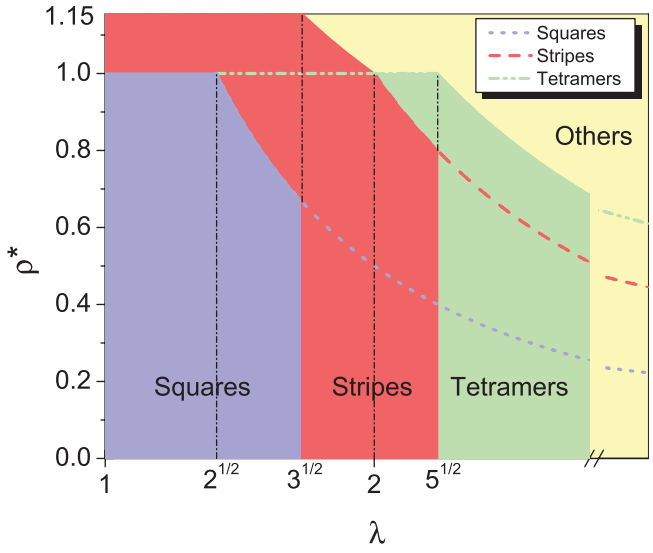

Fig. 3: (Colour on-line) Zero-temperature phase diagram. This figure shows the different regions of the parameter space where different patterns appear. The blue zone represents the region where squares are present; the red zone corresponds to the appearance of stripes; finally, tetrameres appear in the green zone. The yellow zone at the upper-right corner of the figure corresponds to other structures not studied in this work. The blue (dotted line), red (dashed line) and green (dash–double-dotted line) define the maximum density at which squares, stripes, and tetrameres could also appear, respectively, at finite temperatures.

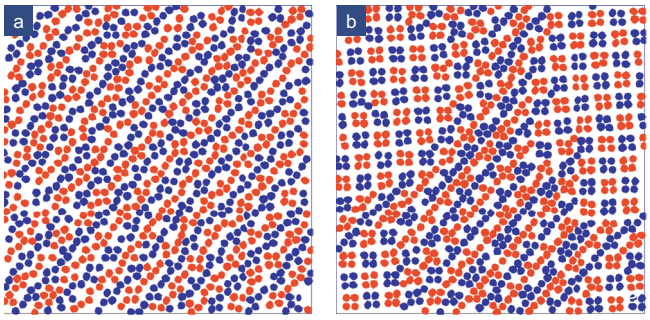

Fig. 4: (Colour on-line) Spatial configurations at temperatures $T^* = 0.5$ and $T^* = 0.1$. Snapshots taken at two temperatures along the annealing isochore for $\lambda = 3$, $\rho^* = 0.65$ and $x = 1$. At high temperatures the system self-assemblies forming fluid-like disordered stripes (a), while at low temperatures the system crystallizes in an ordered square array of tetramers (b).

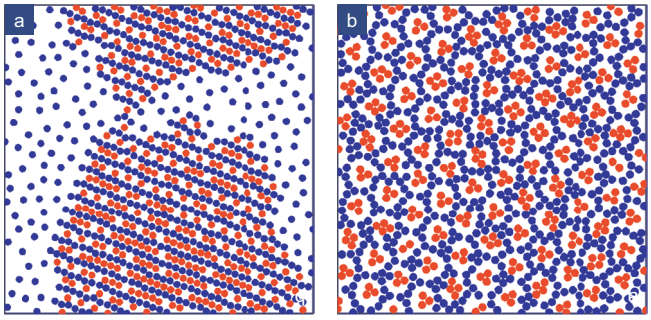

Fig. 5: (Colour on-line) Two representative configurations for asymmetric mixtures ($x = 2$ and $\rho^* = 0.5$). In (a) we observe a phase separation with a region consisting of a high-density blend of the two species and a region consisting of a low-density pure phase of only the majority component, when $\lambda = 1.5$. In (b) we observe the formation of colloidal corrals, where the majority component frames clusters of the minority component when $\lambda = 2$.

Here we see, for instance, that stripes are preferred over squares at larger densities and for a larger range of the coronas, and that tetrameres will be preferred at even larger values of λ. The previous results, obtained using only geometrical arguments, agree with the structures obtained in fig. 2a, b and c; nonetheless, we do not expect an exact correspondence between the phase diagram at $T^* = 0$ with finite-temperature simulations, since in that case entropy plays an important role. This is put in evidence in fig. 2d which shows the square array adopted in a system with the same parameters as in fig. 2b except that the density is reduced to $\rho^* = 0.3$. According to the phase diagram, for this set of parameters one expects the formation of stripes at $T^* = 0$; however, since the square array is less dense, then the particles have more room to vibrate around their equilibrium positions which in turn means that the contribution to the free energy $F = U - TS$ due to the entropy associated with the thermal motion is more important for the square array than for the stripes and therefore the system may adopt the square array. Thus, polymorphic transitions are expected under cooling, specially for parameters near the border of the different regions, *i.e.*, $\lambda \simeq \sqrt{3}$ and $\sqrt{5}$.

Here we are primarily interested in the crystalline configurations that the system may adopt at low temperatures. Nonetheless, the behavior of the system at higher temperatures is also very interesting since under cooling other structures may preempt the crystalline lattice, as previously discussed. In fact, we have found that the original isotropic fluid phase may first suffer a transformation to a disordered fluid-like strip phase. This is exhibited in fig. 4 where snapshots taken at two temperatures along the annealing isochore are shown. Starting with an isotropic fluid phase, as the temperature is decreased the system first shows the formation of a low-temperature fluid phase (panel (a)) consisting of a disordered stripe structure which under further cooling undergoes an abrupt transition at a given temperature from the disordered stripe pattern to a crystalline square array of tetrameres (panel (b)). For the chosen parameters, the array of tetrameres appears to coexist with a stripped structure in which part of the configurational disorder typical of high temperatures remains.

The complexity of the patterns grows with increasing asymmetry in the stoichiometry of the sample. Two representative configurations for non-equimolar mixtures are shown in fig. 5. In panel (a) we observe a phase

separation with a region consisting of a high-density blend of the two species and a region consisting of a low-density phase of the majority component. Lanes similar to those obtained in the equimolar mixture are observed in the high-density component. In general we find that patterns similar to those found for the equimolar mixture appear in the high-density phase. The pure component may also form patterns in the surrounding regions. As expected, the structures found in this pure phase are also similar to those found in a single-component square-shoulder system [13,14]. A different behavior is observed in fig. 5b. Here, there is no macroscopic phase separation; instead, the system exhibits an ordered hexagonal structure consisting of clusters of the minority species corralled by particles of the majority component that form an open network structure. It has been proposed that these morphologies can be employed for the fabrication of nanostructures [1]. For example, after selectively removing one of the blocks, the remaining pattern can be transferred into a functional material [9,19–24]. Similar nanoparticle corrals have recently been obtained in network-self-assembled monolayer hybrid systems [1] and are of particular interest as surface templates because they contain cavities that can be filled by a variety of guest molecules. This kind of open network is particularly flexible since the pore size can be controlled by changing the range of the corona and the asymmetry of the mixture.

It is known that computer simulations risk to be trapped in local energetic minima due to the rough and complex energy landscape [17]; thus, in order to circumvent this problem we have followed a very accurate simulated annealing procedure since for sufficiently slow cooling down of the system one expects that the particles accommodate to its minimum energy configurations when temperature vanishes [25]. Nonetheless, alternative approaches could also be of great help to predict the complete set of ordered equilibrium structures of the system; one of these approaches consists in applying genetic-algorithm search strategies to find in a systematic way minimum energy configurations [26]. Such algorithms have proven to be a reliable way to predict the ordered equilibrium structures for different systems, including monolayers of binary dipolar mixtures [27].

In addition to illustrate the complexity of structures that can arise from the simple model presented in this paper, the system is possible to be carried out experimentally thanks to the recent advances to control colloidal and nanoparticle interactions [8]. From the huge variety of different ordered equilibrium structures developed in the system, here we have shown just a few of them that were chosen due to their possible practical relevance and because some of them have already been observed experimentally [8]. The large versatility of the model indicates that such systems can be adapted to a wide variety of technological applications ranging from the directed growth of molecular wires or carbon nanotubes [15] to nanolithography and nanoelectricity [13] or even as templates for metal deposition.

* * *

We acknowledge partial financial support from grant DGAPA-PAPIIT No. IN-107607.

REFERENCES

[1] Madueno R., Räisänen M. T., Silien C. and Buck M., *Nature*, **454** (2008) 618.
[2] Rechtsman M., Stillinger F. and Torquato S., *Phys. Rev. E*, **73** (2006) 011406.
[3] Rechtsman M., Stillinger F. and Torquato S., *Phys. Rev. E*, **75** (2007) 031403.
[4] Min Y., Akbulut M., Kristiansen K., Golan Y. and Israelachvili J., *Nat. Mater.*, **7** (2008) 527.
[5] Antl L., Goodwin J., Hill R., Ottewill R. and Waters J., *Colloids Surf.*, **17** (1986) 67.
[6] van Blaaderen A. and Vrij A., *Langmuir*, **8** (1992) 2921.
[7] Yethiraj A. and van Blaaderen A., *Nature*, **421** (2003) 513.
[8] Tang C., Lennon E. M., Fredrickson G. H., Kramer E. J. and Hawker C. J., *Science*, **322** (2008) 429.
[9] Bita I., Yang J. K. W., Jung Y. S., Ross C. A., Thomas E. L. and Berggren K. K., *Science*, **321** (2008) 939.
[10] Malescio G., *J. Phys.: Condens. Matter*, **19** (2007) 073101.
[11] Denton A., in *Nanostructured Soft Matter*, edited by Zvelindovsky A. V. (Springer, Dordrecht) 2007, pp. 395–436.
[12] Norizoe Y. and Kawakatsu T., *Europhys. Lett.*, **72** (2005) 583.
[13] Malescio G. and Pellicane G., *Nat. Mater.*, **2** (2003) 97.
[14] Malescio G. and Pellicane G., *Phys. Rev. E*, **70** (2004) 021202.
[15] Camp P. J., *Phys. Rev. E*, **68** (2003) 061506.
[16] Glaser M. A., Grason G. M., Kamien R. D., Kosmrlj A., Santangelo C. D. and Ziherl P., *EPL*, **78** (2007) 46004.
[17] Fornleitner J. and Kahl G., *EPL*, **82** (2008) 18001.
[18] Pauschenwein G. J. and Kahl G., *J. Chem. Phys.*, **129** (2008) 174107.
[19] Mansky P., Chaikin P. and Thomas E. L., *J. Mater. Sci.*, **30** (1995) 1987.
[20] Park M., Harrison C., Chaikin P. M., Register R. A. and Adamson D. H., *Science*, **276** (1997) 1401.
[21] Lammertink R. G. H. *et al.*, *Adv. Mater.*, **12** (2000) 98.
[22] Thurn-Albrecht T. *et al.*, *Science*, **290** (2000) 2126.
[23] Cheng J. Y. *et al.*, *Adv. Mater.*, **13** (2001) 1174.
[24] Jung Y. S. and Ross C. A., *Nano Lett.*, **7** (2007) 2046.
[25] Jagla E. A., *J. Chem. Phys.*, **110** (1999) 451.
[26] Pauschenwein G. J. and Kahl G., *Soft Matter*, **4** (2008) 1396.
[27] Fornleitner J., Lo Verso F., Kahl G. and Likos C. N., *Soft Matter*, **4** (2008) 480.